frontiers | Frontiers in Electronics

TYPE Brief Research Report
PUBLISHED 19 May 2025
DOI 10.3389/felec.2025.1608122

Check for updates

OPEN ACCESS

EDITED BY
Zhenyi Zheng,
National University of Singapore, Singapore

REVIEWED BY
Cuimei Cao,
Huazhong University of Science and Technology, China
Shiwei Chen,
Hubei University, China

*CORRESPONDENCE
Guodong Wei,
jellwei@buaa.edu.cn

RECEIVED 08 April 2025
ACCEPTED 06 May 2025
PUBLISHED 19 May 2025

CITATION
Song X, Cao Z, Bai L, Zhao J, Cai X, Zhu D and Wei G (2025) Interface engineering induced Dzyaloshinskii-Moriya interaction enhancement in Py/Ti/CoFeB/MgO heterostructures.
*Front. Electron.* 6:1608122.
doi: 10.3389/felec.2025.1608122



# Interface engineering induced Dzyaloshinskii-Moriya interaction enhancement in Py/Ti/CoFeB/MgO heterostructures

Xiaoyue Song[1], Zhiqiang Cao[2], Ligang Bai[1], Junbiao Zhao[1,2], Xudong Cai[2], Dapeng Zhu[3] and Guodong Wei[1,2]*

[1]School of Integrated Circuit Science and Engineering, Fert Beijing Institute, Beihang University, Beijing, China, [2]National Key Laboratory of Spintronics, Hangzhou International Innovation Institute, Beihang University, Beijing, China, [3]Integrated Circuit and Intelligent Instruments Innovation Center,Qingdao Research Institute of Beihang University, Qingdao, China

Dzyaloshinskii-Moriya interaction (DMI) is a key driver of chiral magnetism and has garnered significant interest in applied magnetism and spintronics. Interface engineering has been demonstrated to effectively enhance the DMI in many traditional heterostructures. The regulation of DMI is highly dependent on interface properties, which vary significantly across different material systems. Therefore, determining the optimal interface structure to maximize the DMI value presents a complex challenge. In this work, Brillouin light-scattering (BLS) spectroscopy quantitatively reveals a strong interfacial DMI of 17 μJ/m$^2$ in Py/Ti ($t_{Ti}$)/CoFeB/MgO heterostructures with robust perpendicular magnetic anisotropy when the thickness of the Ti layer is 2 nm. Furthermore, we employed a field-modulated magneto-optical Kerr-effect microscope (MOKE) to visualize the existence of stable labyrinth domains in real space in the Py/Ti (2 nm)/CoFeB/MgO systems, which might be able to induce further skyrmions. By optimizing the thickness of a specific membrane configuration, this paper offers a critical materials foundation for advancing spintronics applications.

KEYWORDS

**interface engineering, Dzyaloshinskii-Moriya interaction, heterostructure, magnetic materials, brillouin light scattering, magneto-optical kerr microscope**

## 1 Introduction

In the past decades, the Dzyaloshinskii-Moriya Interaction (DMI) (Fert and Levy, 1980; Crépieux and Lacroix, 1998) has garnered significant interest in applied magnetism and spintronics, such as neuromorphic computing devices, logic devices, two-dimensional materials and high-speed magnetic storage devices (Cao et al., 2018; Kuepferling et al., 2023). The DMI is a kind of asymmetric exchange interaction arising from broken inversion symmetry (Ryu et al., 2013; Emori et al., 2013). In common inversion symmetry breaking systems, such as ferromagnetic and heavy metal (FM/HM) heterojunctions (Kim et al., 2019; Belmeguenai et al., 2015; Yang et al., 2015), DMI can be generated through the strong spin-orbit coupling (SOC) of heavy metals and interfacial symmetry breaking. Additionally, DMI can also be induced in symmetric systems via post-annealing treatments (Ahmadi et al., 2022). These findings have significantly advanced the practical application of DMI in spintronics.

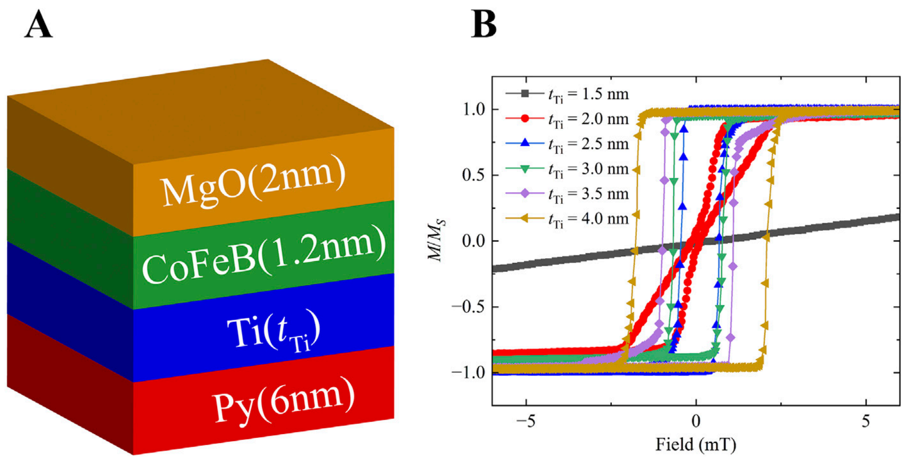


FIGURE 1
**(A)** An illustration of Py/Ti/CoFeB/MgO system. **(B)** The hysteresis loops with perpendicular magnetic field for the multilayer stack with different thicknesses of Ti.

Through strategic interface engineering, we have successfully attained a significant DMI between ferromagnetic materials. This achievement underscores the pivotal role of interface manipulation (Niu et al., 2024) in tailoring magnetic interactions, particularly in heterostructures where symmetry breaking and spin-orbit coupling are meticulously controlled. By optimizing the interfacial properties, the thickness of Ti, we have maximized the DMI magnitude. Here, we propose a materials-optimized heterostructure, Py(6 nm)/Ti ($t_{Ti}$)/CoFeB(1.2 nm)/MgO(2 nm) fabricated through magnetron sputtering, designed to synergistically enhance DMI while maintaining perpendicular magnetic anisotropy (PMA) and interfacial coherence. We present a systematic investigation of interfacial DMI in Py/Ti ($t_{Ti}$)/CoFeB/MgO heterostructures through Brillouin light-scattering (BLS) spectroscopy (Chen et al., 2021; Chen et al., 2024). Quantitative analysis reveals a significant DMI strength of D = 17 μJ/m$^2$ at optimal Ti spacer thickness ($t_{Ti}$ = 2 nm). Subsequently, we fabricated a six-terminal Hall bar device with a Ti layer thickness of 2 nm. We characterized its anomalous Hall effect (AHE) and planar Hall effect (PHE) using an electromagnetic transport system. Crucially, room-temperature labyrinth domain observed by field-modulated magneto-optical Kerr-effect (MOKE) microscopy (Pizzini et al., 2014; Cao et al., 2018), which might be able to induce further skyrmions. These findings position Py/Ti/CoFeB/MgO heterostructures as a versatile materials foundation in the practical application of spintronics.

## 2 Materials and methods

To investigate the emergence and behavior of the DMI in the Py/Ti/CoFeB/MgO heterojunction, we fabricated a series of membrane structures to study how the DMI varies with the thickness of the Ti layer. The thicknesses of the other layers were determined based on prior experimental results. We have meticulously fabricated Py(6 nm)/Ti ($t_{Ti}$)/CoFeB(1.2 nm)/MgO(2 nm)/Ta (2 nm) multilayer heterostructures. The preparation process was carried out with high-precision equipment under highly controlled conditions. The fabrication involved room-temperature magnetron sputtering under ultrahigh vacuum conditions, with a base pressure maintained at 3 × 10$^{-8}$ mbar (equivalent to approximately 3 × 10$^{-6}$ Pa). We grow the samples without an external magnetic field to retain the Py/Ti/CoFeB/MgO heterostructure's native magnetic ordering, ensuring unperturbed spin textures for subsequent analysis. The absence of an additional magnetic field during deposition ensures that the heterojunction retains its intrinsic properties. This fabrication setup is schematically illustrated in Figure 1A.

The heterostructures were grown on thermally oxidized Si/$SiO_2$ substrates via magnetron sputtering physical vapor deposition method, which ensured a reliable foundation for the multilayer structure, facilitating precise control over the growth and quality of the deposited films. We first deposited a 6-nm-thick layer of Py as a ferromagnetic layer. We then grow the Ti layer, ranging from 1.5 nm to 4 nm in thickness, in increments of 0.5 nm, resulting in a total of six samples. The Ti layer can form a good interface interaction with CoFeB, which helps to improve the stability and magnetic properties of the structure. Although the Ti layer itself is paramagnetic, it may indirectly affect the DMI properties of the entire structure by influencing the magnetic anisotropy and spin-orbit coupling of the CoFeB layer. By optimizing the Ti thickness, we achieve a peak DMI energy density. Next, a CoFeB magnetic layer (1.2 nm) with perpendicular magnetic anisotropy was deposited. CoFeB can induce vertical magnetic anisotropy, and the interface with MgO can promote strong spin-orbit coupling and DMI, which are crucial for various spintronic phenomena. These characteristics make it a key material for optimizing device performance and enabling practical applications in spintronics. After the CoFeB ferromagnetic layer, an crystalline MgO tunnel barrier (1.2 nm) was deposited via radio frequency (RF) magnetron sputtering, which provides important support for high performance applications of thin films by enhancing PMA, regulating magnetic coupling and optimizing interface quality. The heterostructure was capped with a 2 nm Ta layer deposited by direct current (DC) sputtering, which serves as the oxidation barrier.

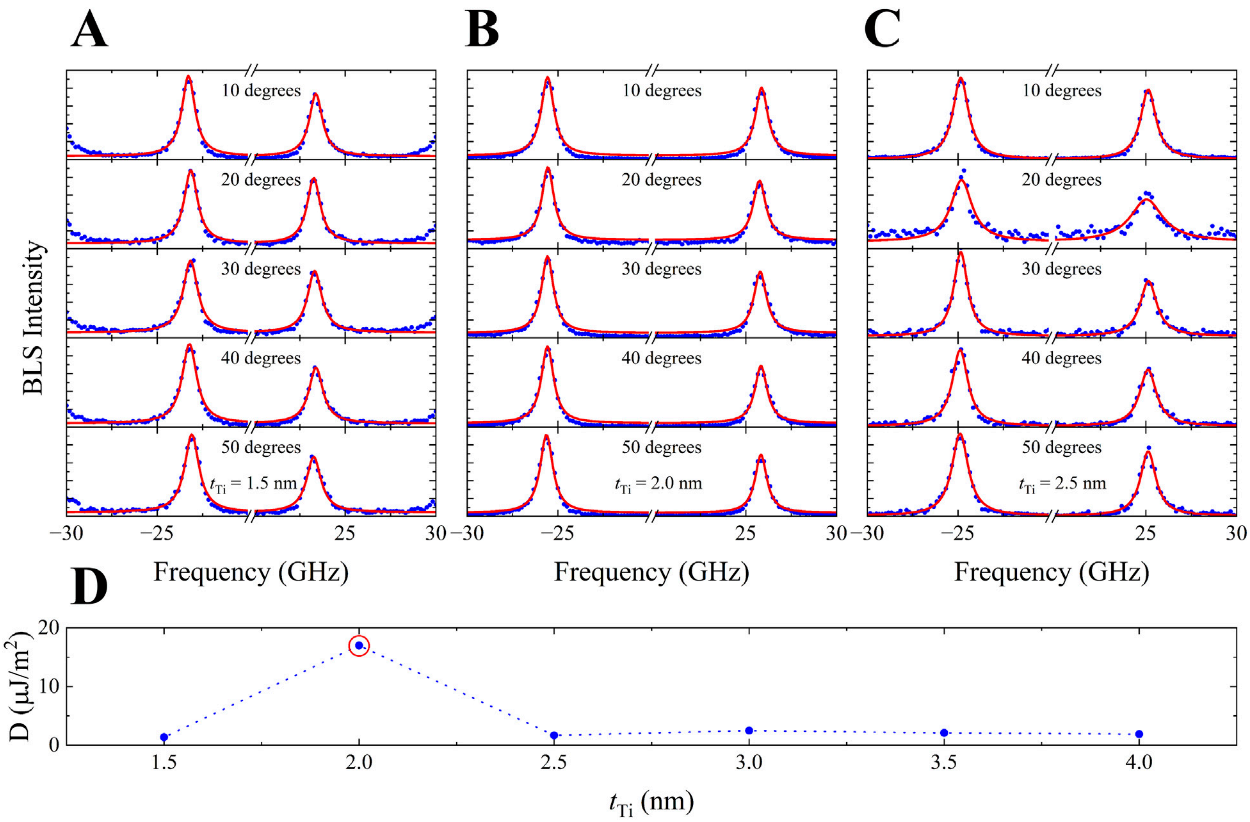


FIGURE 2
A series of BLS spectra obtained by changing wave vectors. Where the blue dots represent the raw data, and the red curve corresponds to the Lorentz fit of the peaks. **(A)** $t_{Ti}$ = 1.5 nm. **(B)** $t_{Ti}$ = 2 nm. **(C)** $t_{Ti}$ = 2.5 nm. **(D)** Py/Ti/CoFeB/MgO style film DMI constant D changing with the thickness of Ti.

In order to improve the magnetic characteristics of the Py/Ti/CoFeB/MgO heterostructures, we performed a post-deposition annealing treatment. All samples with different thicknesses were annealed at 300 ˚C in the presence of a perpendicular external magnetic field of 1 T. The annealing process can enhance the properties of the heterojunction, such as optimizing the PMA and *Ms*. These improvements are attributed to reduced interfacial interdiffusion and stress relaxation. Before proceeding with device fabrication, the heterostructures underwent extensive magnetic characterization. Wafer moke was employed to provide a qualitative assessment of the magnetic properties. Additionally, BLS spectroscopy was utilized for quantitative analysis of the interfacial DMI. Through this series of experiments, we have a certain understanding of the magnetic properties of the heterojunctions.

Subsequently, the heterostructures were patterned into six-terminal Hall bar devices using UV lithography and $Ar^+$ ion milling. The channel dimensions of these devices were precisely defined as 50 μm in width and 500 μm in length. To establish reliable electrical contacts, electron-beam deposition was employed to fabricate Ti/Au (5/100 nm) contacts. Employing Au electrodes can remarkably diminish the electrode resistance, thereby mitigating the energy loss incurred during current transmission. The device configuration enabled the measurement of anomalous Hall effect and allowed for real-time observation of labyrinth domain using polar MOKE microscopy under out-plane magnetic fields (0–5 mT), which might be able to induce further skyrmions, providing a comprehensive understanding of the magnetic behavior under various field conditions.

## 3 Results and discussion

The normalized magnetic hysteresis loops of Py(6 nm)/Ti ($t_{Ti}$)/CoFeB(1.2 nm)/MgO(2 nm)/Ta (2 nm) heterostructures were systematically characterized via wafer moke under sweeping perpendicular magnetic fields. As depicted in Figure 1B, when the thickness of the Ti layer is 1.5 nm, the heterojunction exhibits paramagnetic behavior. Moreover, all heterostructures with Ti spacer thickness $t_{Ti} \geq 2$ nm exhibit well-defined rectangular loops, indicative of robust PMA with coercivity. As shown in the image, the saturation magnetic field of all samples remains consistent, while the coercive force $H_c$ exhibits a growing trend as the thickness of the Ti layer increases.

At a Ti interlayer thickness ($t_{Ti}$) of 2 nm, the magnetic hysteresis loop of the heterojunction system manifests a distinct deviation from the behavior observed in samples with other thickness configurations. Such unique characteristics are hypothesized to originate from the thickness-dependent interfacial DMI, which reaches its maximum strength precisely at this critical thickness. As the Ti layer thickens to $t_{Ti} \geq 2.5$ nm, the DMI intensity decreases. It is shown that the Ti layer thickness can be controlled to construct

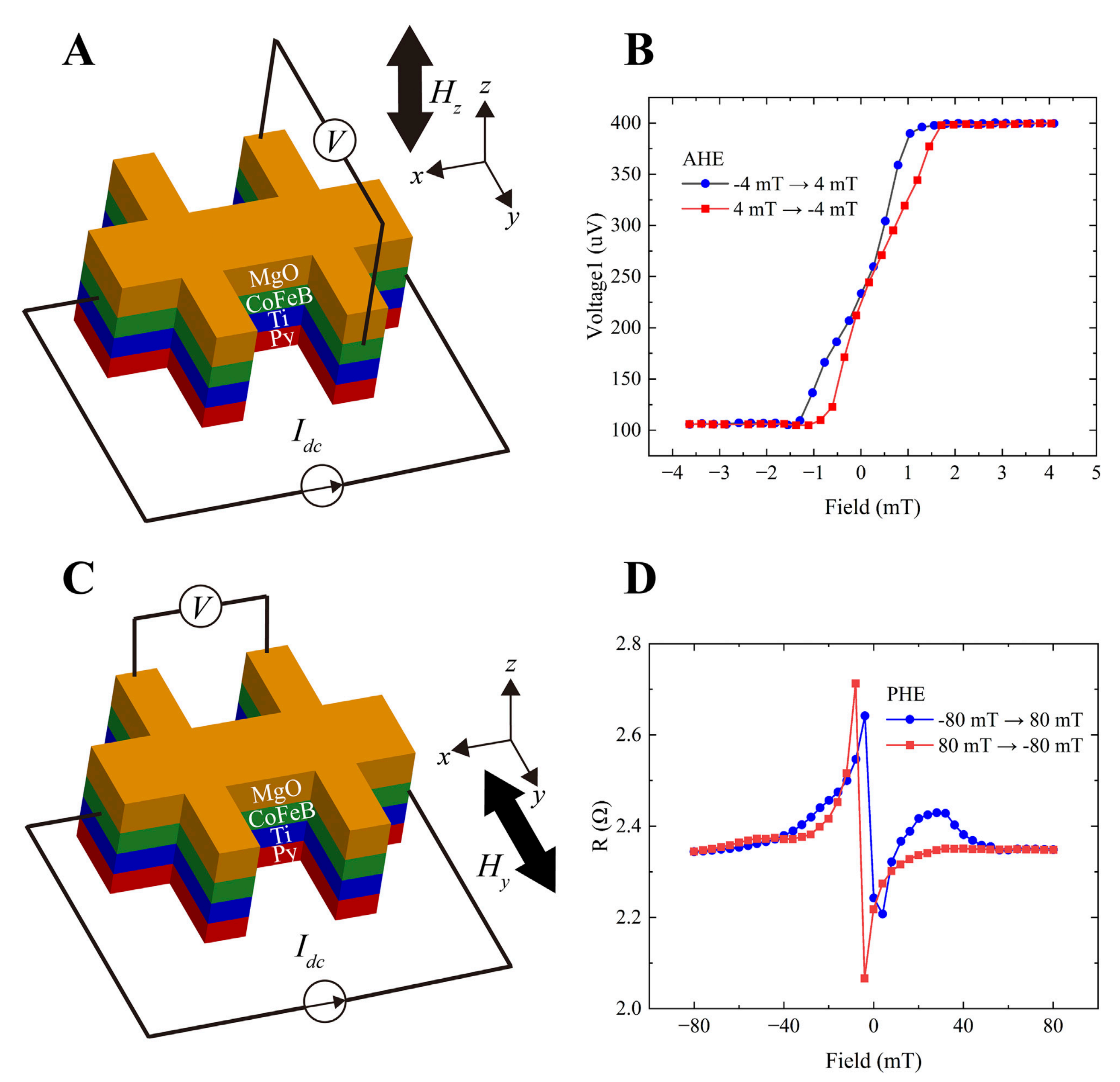


FIGURE 3
**(A)** Schematic illustration of the Hall bar device utilized for probing AHE. **(B)** The hall voltage varies with the vertical magnetic field. **(C)** Schematic illustration of the Hall bar device utilized for probing PHE. **(D)** The magnetoresistance varies with the magnetic field.

the topological magnetic structure. The results reveal the key role of interface engineering: optimizing Ti layer thickness ($t_{Ti} \approx 2$ nm) can synchronically enhance DMI and PMA, which is expected to promote the integrated development in practical applications (Zhang et al., 2024).

Recently, many papers (Udvardi and Szunyogh, 2009; Costa et al., 2010; Cortés-ortuño and Landeros, 2013; Moon et al., 2013) have reported that the non-reciprocal propagation of long-wavelength thermal spin waves (i.e., spin waves traveling in opposite directions have different frequencies) is a significant manifestation of DMI. This non-reciprocity introduces distinct behaviors in spin wave propagation when moving in opposite directions, leading to asymmetric characteristics in the dispersion relationship. This asymmetry can be detected by experimental techniques such as BLS and used to quantify the intensity of DMI. These properties of long wavelength thermal spin waves are important for understanding and designing magnetic structures in spintronics devices. To estimate the interfacial DMI value in Py/Ti ($t_{Ti}$)/CoFeB/MgO heterostructures, we employed BLS spectroscopy with sub-GHz frequency resolution and nanometer-scale surface sensitivity (Nembach et al., 2015) to investigate the asymmetric spin-wave dispersion induced by DMI. A linearly polarized laser beam with a wavelength of 532 nm (Belmeguenai et al., 2015) is focused onto the sample surface. The spin wave dispersion asymmetry, a hallmark of DMI, was systematically mapped by varying the incident laser angle θ (10°–50° in 10° increments) to access wavevectors spanning:

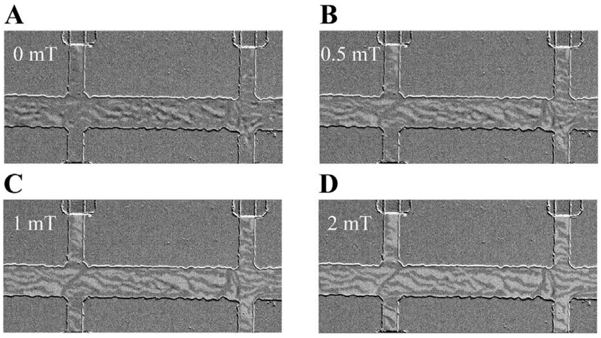


FIGURE 4
Room-temperature labyrinth domains observed by magneto-optical Kerr-effect microscope, taken under different external magnetic field, **(A)** for $H_Z = 0$ mT, **(B)** for $H_Z = 0.5$ mT, **(C)** for $H_Z = 1$ mT, and **(D)** for $H_Z = 2$ mT.

$$k = \frac{4\pi \sin(\theta)}{\lambda}$$

as shown in Figures 2A–C which is the normalized BLS spectrum for as-deposited samples with $t_{Ti} = 1.5$–$2.5$ nm, from where the Stokes and Anti-Stokes peaks can be determined by Lorenz function fitting. Therefore, the frequency difference $\Delta f = f_s - f_{as}$ due to the presence of DMI could be deduced. Furthermore, the DMI energy density D was extracted from the frequency shift $\Delta f$ between counter-propagating spin waves via:

$$\Delta f = \frac{2\gamma D k}{\pi M_s}$$

where $\gamma$ is the gyromagnetic ratio, $k$ is the amplitude of wave vector, and $M_s$ is the saturated magnetization (Di et al., 2015; Ma et al., 2018). By taking $\gamma/2\pi = 31$ GHz/T (Belmeguenai et al., 2015) and $M_s$ measured by VSM into this equation, the DMI energy D can be calculated.

As summarized in Figure 2D, it is clearly depicted the relation of DMI value with Ti layer thickness. The DMI value, denoted as D, shows a pronounced dependence on the thickness of the Ti layer. Specifically, D reaches its maximum value, peaking at $D_{max} = 17$ μJ/m$^2$ for $t_{Ti} = 2$ nm. This peak value indicates that the DMI interaction is most effective at this particular thickness. This highlights the importance of precise thickness control in achieving ideal conditions for such applications.

Figure 3 provides a systematic analysis of the magneto-transport properties of a six-terminal Hall bar device, which is fabricated from the optimized Py(6 nm)/Ti (2 nm)/CoFeB(1.2 nm)/MgO(2 nm) heterostructure. This specifically designed six-terminal Hall bar device is highly suitable for testing the AHE and PHE, as its geometry is precisely engineered to optimize measurements of these phenomena under various magnetic field and charge current conditions. Figure 3A depicts the setup for testing the AHE. As shown, this six-terminal Hall bar device is designed to measure the AHE under the combined influence of an external magnetic field and an applied current. The external magnetic field is oriented along the z-axis, while the current flows along the x-axis. Figure 3B shows the Hall voltage of AHE measured in the presence of an external magnetic field, ranging from −4 to 4 mT. The plot reveals several important characteristics of the heterostructure. Near zero field, the hysteresis loop deviates from the typical rectangular shape, potentially attributed to a large DMI. In contrast, within the saturation field range, the Hall voltage exhibits stability, indicating that the heterojunction possesses significant PMA. This strong PMA is crucial for maintaining the stability of the magnetic properties under varying field conditions.

Figure 3C illustrates the six-terminal Hall bar device designed for characterizing the PHE. The external magnetic field is oriented along the y-axis, while the current flows remain along the x-axis. The PHE represents a pivotal phenomenon within magnetic materials. Figure 3D presents the response of the PHE during a magnetic field reversal. The figure clearly exhibits a significant asymmetry in the magnetoresistance during the experiment. This asymmetry is attributed to the interaction between the Ti and CoFeB surfaces. In summary, the study of both the AHE and the PHE reveals important characteristics of the material, including strong perpendicular magnetic anisotropy, the possible formation of skyrmions, and enhanced spin-orbit interactions. These discoveries play a pivotal role in the progress of next-generation spintronic devices. These devices promise to revolutionize data storage and processing technologies.

Magnetic configuration evolution in Py(6 nm)/Ti (2 nm)/CoFeB(1.2 nm)/MgO(2 nm) heterostructures under perpendicular magnetic fields ($H_z = 0$–$5$ mT) was systematically mapped via polar MOKE microscopy. This technique enables direct observation of magnetic domain reconfiguration dynamics under varying out-of-plane magnetic fields. As illustrated in Figure 4, the magnetic domains exhibit distinct patterns and behaviors as the applied field increases.

Under zero magnetic field, the initial magnetic configuration reveals labyrinth domains, which might be able to induce further skyrmions. This observation indicates that the magnetic structure in this multilayer heterostructure is determined by the delicate interplay between several key interactions: DMI, dipole-dipole interaction, magnetic anisotropy, and exchange interaction (Li et al., 2019). In these interactions, strong DMI is the basis for further observation of skyrmions in Py/Ti/CoFeB/MgO devices at room temperature. This represents a critical step toward energy-efficient beyond-von Neumann computing architectures.

# 4 Conclusion

In summary, we have successfully fabricated a series of Py(6 nm)/Ti ($t_{Ti}$)/CoFeB(1.2 nm)/MgO(2 nm) heterostructures with varying Ti layer thicknesses ($t_{Ti}$) to systematically investigate their magnetic properties. To comprehensively characterize the PMA of these heterostructures, we employed the wafer moke technique. Then, we demonstrated heterostructures exhibit an energy density peaking at D = 17 μJ/m$^2$ for $t_{Ti}$ = 2 nm, as quantified via BLS spectroscopy with sub-GHz resolution. Crucially, we employed MOKE to directly visualize the labyrinth domain structure at room temperature (300 K) under zero external field. These advancements could lead to significant improvements in the speed, energy efficiency, and scalability of spintronic devices, paving the way for innovative applications in high-density magnetic memory, logic gates, and artificial neuromorphic systems.

## Data availability statement

The original contributions presented in the study are included in the article/supplementary material, further inquiries can be directed to the corresponding author.

## Author contributions

XS: Data curation, Formal Analysis, Investigation, Methodology, Validation, Visualization, Writing – original draft. ZC: Formal Analysis, Investigation, Writing – review and editing, Conceptualization, Methodology. LB: Writing – review and editing, Formal Analysis, Investigation. JZ: Resources, Supervision, Writing – review and editing. XC: Investigation, Project administration, Resources, Supervision, Writing – review and editing. DZ: Funding acquisition, Project administration, Writing – review and editing. GW: Data curation, Investigation, Writing – original draft, Writing – review and editing, Conceptualization, Funding acquisition, Project administration.

## Funding

The author(s) declare that financial support was received for the research and/or publication of this article. This work was supported by the Key R&D Plan of Shandong Province (2022CXGC020208), the National Natural Science Foundation of China (52261145694, 92164206, W2411060, 62274009, 52003014), the Beijing Municipal Natural Science Foundation (Z230004) and Taishan Scholars Program.

## Conflict of interest

The authors declare that the research was conducted in the absence of any commercial or financial relationships that could be construed as a potential conflict of interest.

## Generative AI statement

The author(s) declare that no Generative AI was used in the creation of this manuscript.

## Publisher's note



## References

Ahmadi, K., Mahfouzi, F., Jamilpanah, L., Mohseni, M., Böttcher, T., Pirro, P., et al. (2022). Inducing Dzyaloshinskii–Moriya interaction in symmetrical multilayers using post annealing. *Sci. Rep.* 12 (1), 11877. doi:10.1038/s41598-022-16244-w

Belmeguenai, M., Adam, J., Roussigné, Y., Eimer, S., Devolder, T., Kim, J., et al. (2015). Interfacial Dzyaloshinskii-Moriya interaction in perpendicularly magnetized ultrathin films measured by Brillouin light spectroscopy. *Phys. Rev. B* 91 (18), 180405. doi:10.1103/PhysRevB.91.180405

Cao, A., Zhang, X., Koopmans, B., Peng, S., Zhang, Y., Wang, Z., et al. (2018). Tuning the Dzyaloshinskii–Moriya interaction in Pt/Co/MgO heterostructures through the MgO thickness. *Nanoscale* 10 (25), 12062–12067. doi:10.1039/c7nr08085a

Chen, R., Cao, A., Wang, X., Liu, Y., Yang, H., and Zhao, W. (2024). Oscillation of Dzyaloshinskii–Moriya interaction driven by weak electric fields. *Chin. Phys. B* 33 (2), 027501. doi:10.1088/1674-1056/ad0f85

Chen, R., Wang, X., Cheng, H., Lee, K., Xiong, D., Kim, J., et al. (2021). Large Dzyaloshinskii-Moriya interaction and room-temperature nanoscale skyrmions in CoFeB/MgO heterostructures. *Cell Rep. Phys. Sci.* 2 (11), 100618. doi:10.1016/j.xcrp.2021.100618

Cortés-ortuño, D., and Landeros, P. (2013). Influence of the Dzyaloshinskii–Moriya interaction on the spin-wave spectra of thin films. *J. Phys. Condens. Matter* 25 (15), 156001. doi:10.1088/0953-8984/25/15/156001

Costa, A. T., Muniz, R. B., Lounis, S., Klautau, A. B., and Mills, D. L. (2010). Spin-orbit coupling and spin waves in ultrathin ferromagnets: the spin-wave Rashba effect. *Phys. Rev. B* 82 (1), 014428. doi:10.1103/PhysRevB.82.014428

Crépieux, A., and Lacroix, C. (1998). Dzyaloshinsky–Moriya interactions induced by symmetry breaking at a surface. *J. Magnetism Magnetic Mater.* 182, 341–349. doi:10.1016/S0304-8853(97)01044-5

Di, K., Zhang, V. L., Lim, H. S., Ng, S. C., Kuok, M. H., Yu, J., et al. (2015). Direct observation of the dzyaloshinskii-moriya interaction in a Pt/Co/Ni film. *Phys. Rev. Lett.* 114 (4), 047201. doi:10.1103/PhysRevLett.114.047201

Emori, S., Bauer, U., Ahn, S., Martinez, E., and Beach, G. S. D. (2013). Current-driven dynamics of chiral ferromagnetic domain walls. *Nat. Mater.* 12 (7), 611–616. doi:10.1038/nmat3675

Fert, A., and Levy, P. M. (1980). Role of anisotropic exchange interactions in determining the properties of spin-glasses. *Phys. Rev. Lett.* 44, 1538–1541. doi:10.1103/PhysRevLett.44.1538

Kim, D., Haruta, M., Ko, H., Go, G., Park, H., Nishimura, T., et al. (2019). Bulk Dzyaloshinskii–Moriya interaction in amorphous ferrimagnetic alloys. *Nat. Mater.* 18 (7), 685–690. doi:10.1038/s41563-019-0380-x

Kuepferling, M., Casiraghi, A., Soares, G., Durin, G., Garcia-sanchez, F., Chen, L., et al. (2023). Measuring interfacial Dzyaloshinskii-Moriya interaction in ultrathin magnetic films. *Rev. Mod. Phys.* 95 (1), 015003. doi:10.1103/RevModPhys.95.015003

Li, W., Bykova, I., Zhang, S., Yu, G., Tomasello, R., Carpentieri, M., et al. (2019). Anatomy of Skyrmionic Textures in Magnetic Multilayers. *Adv. Mater.* 31 (14), e1807683. doi:10.1002/adma.201807683

Ma, X., Yu, G., Tang, C., Li, X., He, C., Shi, J., et al. (2018). Interfacial dzyaloshinskii-moriya interaction: effect of band filling and correlation with spin mixing conductance. *Phys. Rev. Lett.* 120 (15), 157204. doi:10.1103/PhysRevLett.120.157204

Moon, J., Seo, S., Lee, K., Kim, K., Ryu, J., Lee, H., et al. (2013). Spin-wave propagation in the presence of interfacial Dzyaloshinskii-Moriya interaction. *Phys. Rev. B* 88 (18), 184404. doi:10.1103/PhysRevB.88.184404

Nembach, H. T., Shaw, J. M., Weiler, M., Jué, E., and Silva, T. J. (2015). Linear relation between Heisenberg exchange and interfacial Dzyaloshinskii–Moriya interaction in metal films. *Nat. Phys.* 11 (10), 825–829. doi:10.1038/NPHYS3418

Niu, H., Kwon, H. Y., Ma, T., Cheng, Z., Ophus, C., Miao, B., et al. (2024). Reducing crystal symmetry to generate out-of-plane Dzyaloshinskii–Moriya interaction. *Nat. Commun.* 15 (1), 10199. doi:10.1038/s41467-024-54521-6

Pizzini, S., Vogel, J., Rohart, S., Buda-prejbeanu, L. D., Jué, E., Boulle, O., et al. (2014). Chirality-induced asymmetric magnetic nucleation in Pt/Co/$AlO_x$ ultrathin microstructures. *Phys. Rev. Lett.* 113 (4), 047203. doi:10.1103/PhysRevLett.113.047203

Ryu, K., Thomas, L., Yang, S., and Parkin, S. (2013). Chiral spin torque at magnetic domain walls. *Nat. Nanotechnol.* 8 (7), 527–533. doi:10.1038/nnano.2013.102

Udvardi, L., and Szunyogh, L. (2009). Chiral asymmetry of the spin-wave spectra in ultrathin magnetic films. *Phys. Rev. Lett.* 102 (20), 207204. doi:10.1103/PhysRevLett.102.207204

Yang, H., Thiaville, A., Rohart, S., Fert, A., and Chshiev, M. (2015). Anatomy of dzyaloshinskii-moriya interaction at Co/Pt interfaces. *Phys. Rev. Lett.* 115 (26), 267210. doi:10.1103/PhysRevLett.115.267210

Zhang, Y., Tang, J., Wu, Y., Shi, M., Xu, X., Wang, S., et al. (2024). Stable skyrmion bundles at room temperature and zero magnetic field in a chiral magnet. *Nat. Commun.* 15 (1), 3391. doi:10.1038/s41467-024-47730-6